FIRE BEHAVIOR IN NONUNIFORM FUELS

WILLIAM H. FRANDSEN
PATRICIA L. ANDREWS

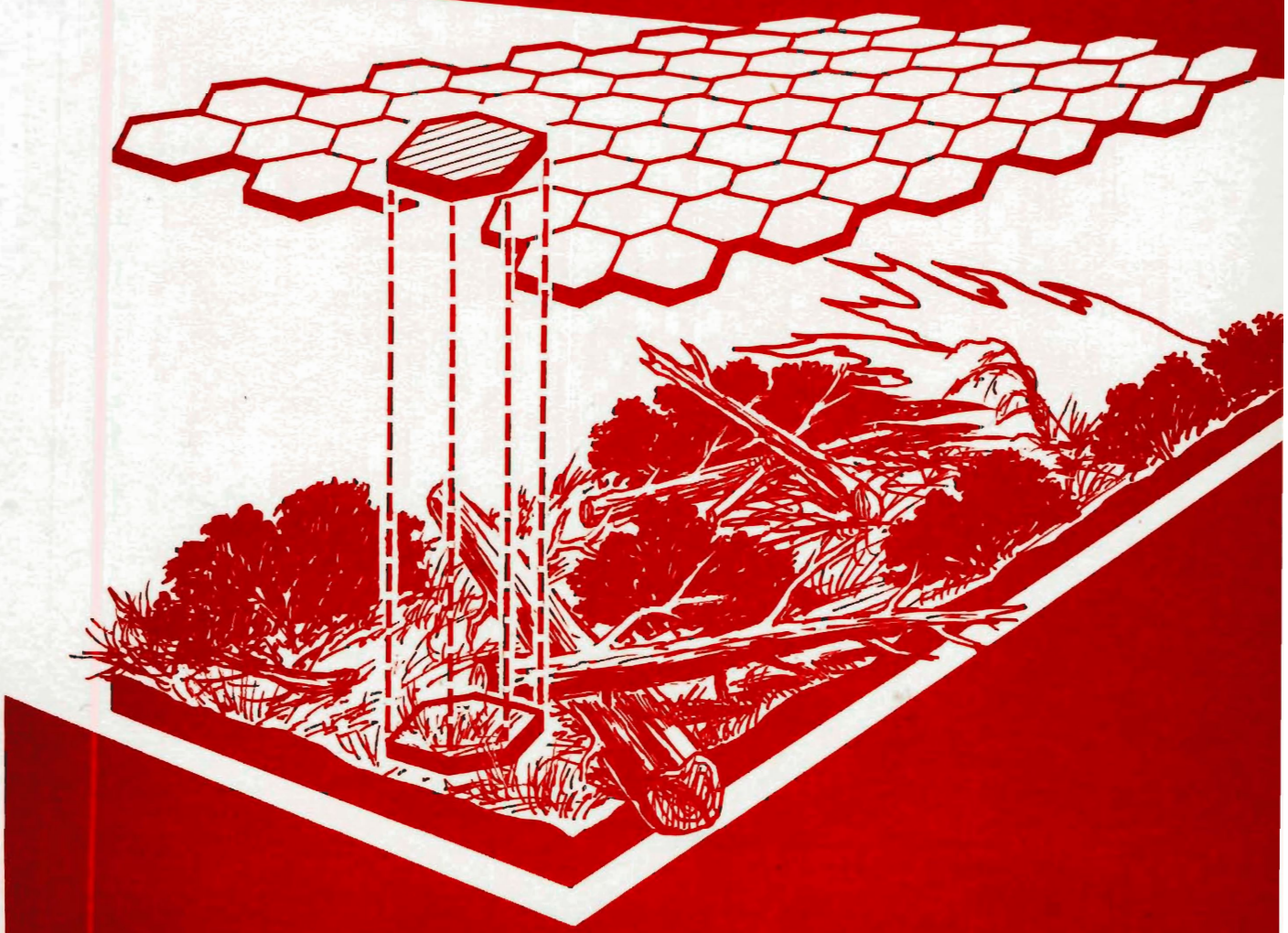

USDA Forest Service Research Paper INT-232
Intermountain Forest and Range Experiment Station
Forest Service, U.S. Department of Agriculture

USDA Forest Service
Research Paper INT-232
August 1979

FIRE BEHAVIOR IN NONUNIFORM FUELS

William H. Frandsen
and
Patricia L. Andrews

INTERMOUNTAIN FOREST AND RANGE EXPERIMENT STATION
Forest Service
U.S. Department of Agriculture
Ogden, Utah 84401

THE AUTHORS

WILLIAM H. FRANDSEN is a Research Physicist stationed at the Northern Forest Fire Laboratory in Missoula, Montana. He received his B.A. in physics and mathematics from Lewis and Clark College in 1954, and his M.A. in physics from the University of Oregon in 1960. Frandsen was employed from 1955-1967 as a physicist at the Naval Weapons Center at China Lake, California. While there, he was involved in two fields of study: infrared detection systems and the effects of ultrasound on metals. Since 1967, Frandsen has been with the Fire Fundamentals research work unit at the Northern Forest Fire Laboratory, where he is responsible for the technical planning and execution of research concerned with the thermodynamics of the fire and its interaction with the fuel complex.

PATRICIA L. ANDREWS is a Mathematician stationed at the Northern Forest Fire Laboratory in Missoula, Montana. She received her B.A. in mathematics and chemistry from Eastern Montana College in 1970, and her M.A. in mathematics and computer science from the University of Montana in 1973. Andrews has been with the Fire Fundamentals research work unit at the Northern Forest Fire Laboratory since 1973.

ACKNOWLEDGMENTS

The authors wish to thank all of their project co-workers for many helpful suggestions. Special thanks goes to project leader Richard Rothermel for support and encouragment, and colleague Frank Albini for constructive criticism and suggestions. Thanks also goes to Mike Marsden for the helpful discussions on the simulation of fuel arrays and to Roger McClusky for developing those ideas into a computer program.

ERRATA

Frandsen, William H. and Patricia L. Andrews. 1979. Fire behavior in nonuniform fuels. Res. Pap. INT-232. Ogden, UT: U.S. Department of Agriculture, Intermountain Forest and Range Experiment Station. 34 p.

Page 21: A reference was left out of the Publications Cited.

Sneeuwjagt, Richard J. 1974. Evaluation of the grass fuel model of the National Fire Danger Rating System. MS. Thesis. Seattle, WA: University of Washington. 162 p. Thesis.

Page 27: Equation (14a). A "/" was left out.

$$t = \begin{cases} \left[-C + \sqrt{C^2 + 2B(1-C)}\right] / [(1-C)/(\tau_r)_{i+1}], & \text{for } 0 < s \leq D' \quad (14a) \\ (s - D')/R + (\tau_r)_{i+1}, & \text{for } D' < s \leq D \quad (14b) \end{cases}$$

Page 28: An "s" should be "≤"

or for D'>D and $0<\theta\leq\tau_r$

RESEARCH SUMMARY

Predicting fire behavior in nonuniform fuel arrays is a problem requiring:

1. A method of assessing fuel nonuniformity,
2. A method of simulating fuel nonuniformity, and
3. An algorithm governing fire spread through a simulated array.

Satisfying these requirements is the objective of this paper. The main concept is built around partitioning the fuel into a honeycomb array. Each cell is described independently according to its bulk fuel parameters (depth, load, average particle size, etc.). Field assessment is designed to meet the requirements of simulation. An algorithm simulates fire spread through the array by coupling predictions of heat flowing from a burning cell to predictions of the heat required for ignition of the adjacent cells. Ignition is allocated to the cell offering the least requirement for heat. Consequently, the fire moves nonuniformly through the array taking advantage of the path of least resistance. Methodology is emphasized.

A simulated fire is initiated from a line source. Distortions in the propagating front result from fuel nonuniformities giving rise to a distribution of rates of spread rather than a single value. Analysis is appropriate for an assessment of a distribution of the fireline intensities.

Examples are given for slash, residue after tree harvest, and a mixture of grass and sagebrush. Nominal windspeeds of 0 and 2 mi/h were chosen for the purpose of illustrating the technique for handling nonuniformity.

Comparisons show that the previous alternative of combining all fuel to an average depth and load does not allow the land manager to assess the chance that patches of high risk fuel arrangements might result in unacceptable fire behavior.

CONTENTS

Page

INTRODUCTION 1

SIMULATING FIRE BEHAVIOR 4

Fuel Array Assessment 7

SLASH 7
GRASS AND SAGEBRUSH 11

Fuel Array Generation 12

SLASH 12
GRASS AND SAGEBRUSH 14

RESULTS 15

Slash 15

Grass and Sagebrush 18

DISCUSSION 19

PUBLICATIONS CITED 20

NOMENCLATURE 22

APPENDIX I. DELAY TIME 23

APPENDIX II. CELL BURNING FRACTION 28

APPENDIX III. CELL LOAD EVALUATION 29

APPENDIX IV. EVALUATING b_o, b_1, b_2 AND b_3 29

APPENDIX V. ERROR TERM 34

INTRODUCTION

Fire behavior in a woody fuel array such as found in the forest is a complex physicochemical process that does not lend itself to a simple solution. The process is further complicated by the spatial nonuniformity of the fuels involved in the combustion process. A fire responds to fuel nonuniformity by changing its rate of spread and intensity. As a result there is a distribution in the rate of spread and intensity experienced by the fire as it spreads through the fuel array.

For the purposes of this study nonuniform fire behavior is predicted by modeling fire spread through a hexagonal network of fuel cells. Fire spread is assumed to be a process of contagious growth between cells. Fuel properties are allowed to vary from cell to cell in a prescribed manner but have uniform properties within the cell. Consequently, the nonuniformity of the actual fuel array is simulated through cell to cell variations and has a resolution limited by the cell size. Because of the nature of the modeling process it is necessary to devise a scheme for collecting data describing nonuniformity and a scheme for filling the hexagonal cell array in a manner that simulates the actual fuel nonuniformity.

Historically, it was necessary that uniformity be addressed first. This approach laid the groundwork for present development. Rothermel (1972) chose a path of research into fire behavior that allowed the result to be applied to the needs of the fire manager. Rothermel's variables were the fuels and the environment in which they were found. That same view exists here. The fundamental approach of the model described here is the assumption that small portions of a nonuniform fuel bed can be considered uniform. Nonuniform fire behavior then can be examined by following the progress of the fire as it changes speed while moving through different but uniform subunits of the area. This model was developed as part of an integrated effort for solving fire behavior problems at the Northern Forest Fire Laboratory. The model is not intended for direct simulation of actual fire situations but rather is offered as a means to develop simplified methods for solving fire behavior problems in the field.

Some aspects of fuel nonuniformity such as occasional absences of fuel have a direct effect on fire behavior. However, most often fuel nonuniformities are more subtle and must be viewed through another interpretive system, a model of fire behavior. Consequently, we define fuel nonuniformity in terms of fire nonuniformity through a model of fire behavior that responds to spatial variations of the fuel array.

Uniform fuel arrays and uniform fires do not occur. All fire behavior in woody fuel arrays is nonuniform. Fire behavior becomes uniform by definition. As a point of comparison, most people consider fire spreading over a sheet of paper as uniform. But, it may be viewed by some as nonuniform by focusing on the elemental combustion process. Certainly, fuel uniformity does not exist in natural woody fuel arrays. The arrays are comprised of separated particles. Fons (1946) described fire spread as a series of ignitions. Fire spread appears to follow this description on the scale of the fuel separation. The flame ignites the particle and then spreads along that particle until it reaches another particle. The flame may ignite the next particle by flame contact or the particle may ignite after radiation from the flame front has preheated the fuel sufficiently to drive off combustible gases that burn when in contact with flame.

A fire appears uniform when the particle separation is small compared to the flame size (or the range of influence of the flame). Individual flames coalesce into a solid moving front and the fire spreads in response to the bulk fuel properties of the array--load, particle size distribution, and depth. These properties are defined within a volume element, averaging out the small variations of particle separation. Averaging is not limiting so long as the volume element encountered by the flame is small compared to the size or range of influence of the flame. It is this level of nonuniformity that we address. Wind and slope can act to increase the size of the flame and orient it so that the spatial variation of bulk fuel properties is small compared to the area affected by the flame. Thus, a nonuniform fire can become uniform in the presence of wind or slope.

Although resolution is limited by the cell size, the introduction of wind alters the overall perspective of resolution. Wind increases the size of the area sustaining active combustion and therefore increases the error of locating the fire. Consequently, in the presence of wind, the size of the cell can be increased without altering accuracy in locating the fire.

The model is applied to two examples of nonuniformity: slash, residue left after tree harvesting, and a mixed community of grass and sagebrush. (Slash is more uniform than a mixed community of grass and brush.) The reader should expect to gain an appreciation for the problem of defining fire nonuniformity, developing a model of fire behavior that responds to fuel nonuniformity, and an appreciation of the kind and form of the results obtained from the nonuniformity model. Attempts are not made to validate the model. Consequently, the rigors of replication are replaced with a logical flow of fire behavior concepts--concepts derived from the uniform fire behavior model. The initial advantage is a consistent manner of handling field data that is applied to nonuniform fire behavior.

The response of a spreading fire to the bulk properties of woody fuel arrays--as found in forest fuels--has been investigated by Fons (1946), Thomas and Simms (1963), Anderson (1968, 1969), Frandsen (1971), Steward (1971), and Rothermel (1972). Rothermel incorporated fuel parameters (load, size, depth) and the fuel interactions into a model of fire spread through a continuous fuel array. Although the fuel array is continuous, it may be heterogeneous in size and type. Live and dead fuel may be included if mixed in the same stratum.

Fuel parameters for the uniform fire spread model are categorized as living or dead, and averaged within a specific set of fuel size classes. The fuel array is assumed to be continuous. As a consequence, the model given by Rothermel (1972) predicts well for spatially continuous fuels and becomes increasingly less accurate as fuel discontinuity increases. To properly assess fire behavior, continuity must be included as an essential parameter in the mechanism of fire spread. Brown (1966) described the problem of continuity as follows:

Closely related to compactness but on a larger scale is continuity or patchiness of fuels. It represents the degree of change, horizontally and vertically, in the physical characteristics of fuels existing over a given area and is a measure of the uniformity of continuous combustion (for a constant set of weather conditions). At present, a meaningful quantitative description of continuity is lacking. Development of an objective description of continuity would be of benefit to continued fire research as well as fuel appraisal and fire control planning.

A discontinuous fuel array exhibits abrupt changes and is a unique example of nonuniformity. We employ a broad definition of nonuniformity that includes discontinuities.

A simple example of a nonuniform array is one in which only the depth varies. The fire cannot achieve a constant rate of spread throughout the entire fuel complex, but may achieve it for some uniform subunit of the larger nonuniform array. Consequently, fire will accelerate and decelerate as it moves through the array. An observer usually calculates the average rate of spread from the time it takes the fire front to travel some given distance, but the result may not be related to either the individual depths or to the average depth.

Nonuniform fire behavior implies more than one result for the rate of spread and intensity. Results should be expressed as a frequency distribution allowing the user more complete information on which to base a decision. The breadth of the distribution indicates the range of options to be considered in the management or control of a fire. Rothermel (1974) gives general accuracy requirements for the application of fire behavior models to fire management and control ranging from training aids to real-time fire predictions. As a training aid the new information will help emphasize the probabilistic nature of fire behavior. The impact on planning and management can be profound allowing a realistic assessment of the range of effects for alternative treatments of the land. The highest requirement for accuracy is predicting real-time fire behavior. A knowledge of fire nonuniformity at this stage is essential.

A method of collecting information from the field that represents fuel nonuniformity is not common to present fuel inventory systems. Use of average fuel parameters in the uniform model as an alternative produces less reliable results as the fuel array becomes more nonuniform. An averaging of the fuel parameters prior to processing by a fire behavior model ignores the variable nature of fire as it moves through a nonuniform fuel array. A change in the fuel does not imply a proportional change in the fire behavior. An improved estimate of fire behavior can be derived from an analysis of the distribution of fire characteristics produced by the model as the fire passes through the array.

Both rate of spread and intensity are implied in the frequency distributions of fire behavior results. Distributions of the rate of spread allow for a realistic assessment of the actual range of spread rates and area growth rates essential to prescribed burning and the control of wildfire. Distributions of the fire intensity provide insights for an assessment of the distributions of flame lengths and crown scorch heights to be expected on a site. As research into quantification of the heat pulse impinging on the site progresses and is related to the intensity distribution, assessment of the proportion of the burned area that will regenerate vegetation after a fire should be possible. Variation in regeneration is seen in the response of seedlings in the vicinity of pile burning. Davis (1959) writes:

It is common to observe that seedlings and other vegetation often do not become established for several years where large slash piles have been burned. A profusion of vegetation may fringe the area, but the center may be bare.

These efforts also should provide inputs to hydrologic and soil stability impacts.

SIMULATING FIRE BEHAVIOR

We are concerned only with nonuniform fire spread in the horizontal plane. Arrays with large vertical nonuniformity are not considered. The results of the simulation must reflect the variability in fire behavior due to the spatial nonuniformity of the fuel. Fire spread results are presented as a frequency distribution of the rate of spread of the fire front at variable lapsed times from ignition of the initial fire front. Intensity distributions are presented for those lapsed times.

The simulated fuel bed consists of an array of cells. Each cell is described by a set of basic fuel parameters (Rothermel 1972) that affect the rate of fire spread. The time to move from cell to cell depends on the parameters of the two adjacent cells. The fuel is assumed to be evenly distributed within each cell.

The fire begins as a line source and travels from cell to cell by contagious growth through a series of ignitions and spreads at a rate based on a minimum delay time (appendix I) within each individual cell (fig. 1). Hexagonal cells are used because they do not have point contacts when arranged in an array and offer the maximum number (six) of growth directions while maintaining a constant distance between cell centers.

The delay time is the core of this analysis. Delay time is viewed as the time it takes for the fire to spread through the cell. Thus it is the amount of time the fire is delayed in a cell before it can attack an adjacent cell. The delay time is the sum of two parts: the time to achieve the quasi-steady spread rate in the cell and the time to spread the remaining distance at a steady rate of spread. The time to reach the quasi-steady state is assumed to be the residence time of the cell and the remaining time is the remaining distance divided by the quasi-steady rate of spread for that cell. Consequently, the cell chosen must be of a size such that the time for the fire to spread through the cell is equal to or greater than the residence time of the fire in the cell. An essential restriction of the model is that the influence from a burning cell extend no further than its immediate neighbors.

After passage of the front, the fire will remain burning in the cell for a period of time dependent on cell fuel properties, the properties of the cell it was ignited by, and the size of the fuel cell. The delay time can be shortened after ignition if heat from another adjacent cell has sufficient intensity to offer a delay time less than the present waiting time.

Fire from one cell can ignite an adjacent cell after it has reached its escape level, i.e. waited a time equivalent to its delay time. If the adjacent cell is presently unignited, the fire moves in, delay time is assigned, and the fire begins its waiting period to reach its escape level. If the adjacent cell is already ignited and the proposed delay time is less than the present waiting time, then the waiting time is replaced by the delay time. Otherwise the cell retains its waiting time. A detailed discussion of the delay time appears in appendix I.

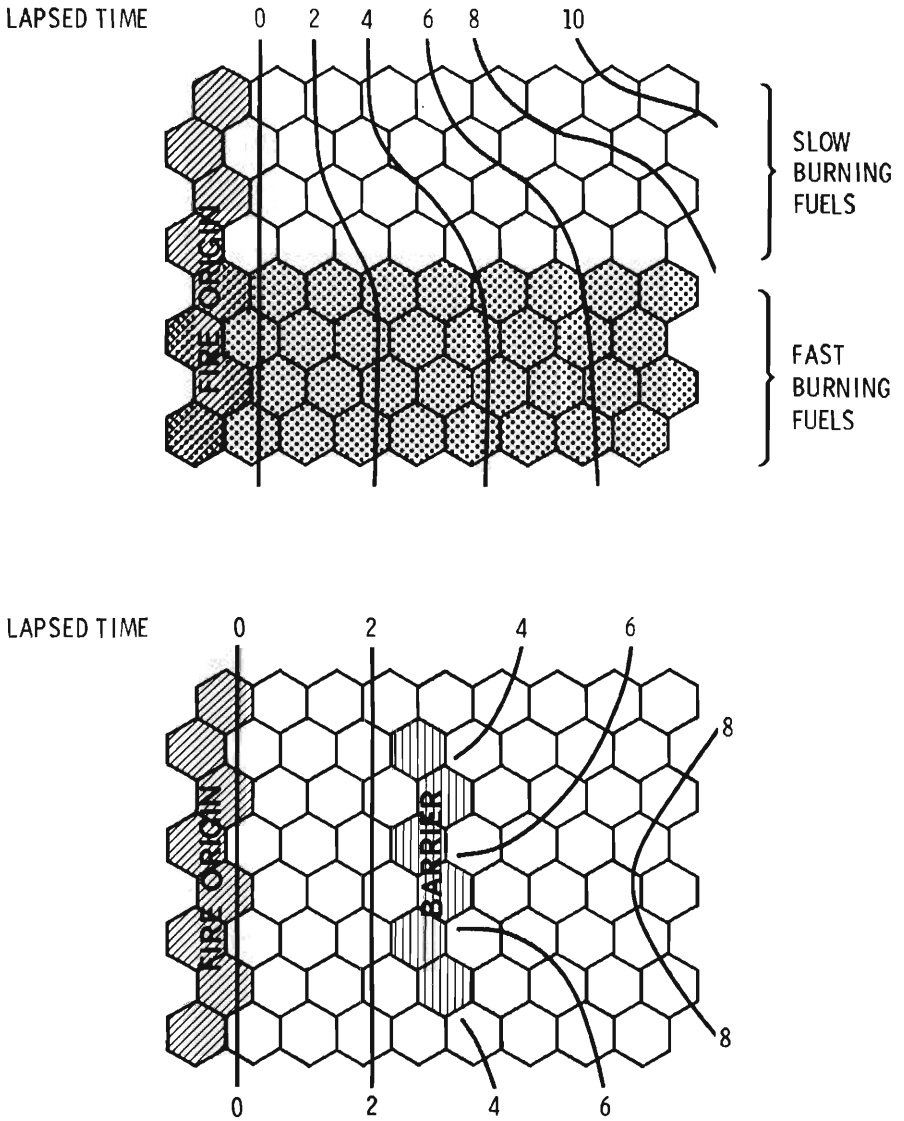

Figure 1.--Fire front progress through two nonuniform hexagonal fuel arrays.

The rate of fire spread also has a dependence on wind and slope. Rothermel (1972) used only the maximum effect, i.e. wind and slope in the same direction. Provision was not made for combining nonparallel wind and slope nor for the computation of rates of spread in the six spread directions required by the hexagonal array. Albini,[1] however, developed a method for combining wind and slope that gave the resultant magnitude of rate of spread as a function of an angle relative to the directions of the wind and slope. With Albini's model, it was possible to compute potential rates of spread in all six directions in the presence of wind and slope.

---

[1]Albini, Frank A. Memorandum, subject, Combining wind and slope effects on spread rate, to R. C. Rothermel, Northern Forest Fire Laboratory, Missoula, Montana 59806, Jan. 19, 1976.

As a comparison, the Dijkstra (1959) algorithm employed in the Kourtz-O'Regan (1971) fire spread model locates the paths of least resistance based on delay times dependent only on the fuel descriptors of each individual cell, without dependence on an adjacent cell. As each cell is reached--ignited--by the fire, the lapsed time since fire starting time is recorded in the cell. Isochrones can then be drawn to illustrate the progress of the fire. The two models are similar except for the differences in delay time mentioned above. The Dijkstra model does not require updating since it maps the path of least resistance to fire spread. Presently the Kourtz-O'Regan model uses very large cells and average fuel parameters to describe the average rate of spread and thus the delay time to consume the fuel cell. The hexagonal model operating on cells that are subunits of the larger Kourtz-O'Regan cell then can provide a distribution of rate of spread values needed to compute the probable time a fire takes to consume a cell in the Kourtz-O'Regan model. Thus, data obtained from the hexagonal model could be used as input to the Kourtz-O'Regan model.

For a continuous fuel array the fireline intensity is the product of the reaction intensity and the combustion zone depth (Albini 1976) and assumes a constant reaction intensity throughout the combustion zone. For the nonuniform array the reaction intensity is assumed constant throughout the cell but may vary from cell to cell.

Following a suggestion by Frank Albini of the Northern Forest Fire Laboratory, the fireline intensity is obtained by summing the products of the reaction intensity and that portion of the cell contributing to the combustion process. Each column is scanned perpendicular to the initial fire front (fig. 1):

$$I_B = \sum_i (I_R)_i F_i D$$

where I_B is the column fireline intensity, $(I_R)_i$ is the reaction intensity of the i^{th} cell, F_i (appendix II) is that fraction of the i^{th} cell that is contributing to the combustion process, and D is the cell width. All column intensities then are grouped to form a frequency distribution.

The sum of the products, $\sum_i F_i D$, is the combustion zone depth if the fire is burning perpendicular to the initial line of fire. Occasionally, portions of the fire front may be burning to the side. Scanning down the columns would then give some combustion zone depths that are unreasonably high. This results in spikes in the distribution at high fireline intensities that can be easily located and disregarded.

Fuel Array Assessment

The geometric nature of the fire behavior model presented resulted in a fire spread algorithm coupled to a hexagonal array of fuel cells. However, application to the field is not possible unless we are able to fill the hexagonal array in a manner that preserves the horizontal stratification of the actual fuel array. Filling the hexagonal cells requires fuel array data (load, size, depth) that must be acquired in a manner that fills the needs of the cell filling algorithm. In general, we should look for some classifiable character to give the assessed nonuniformity a recognizable distinction related to its habitat type or other comparable classification, i.e., fuel type, and age. Habitat classification according to Daubenmire and Daubenmire (1968) is presently used by the USDA Forest Service in Idaho and Montana to classify vegetation and its associated environment. Fuels are a byproduct of the habitat type but may occur in different arrangements of load, particle size distribution, and depth, and thus are classified separately. Fuel models used in the U.S. National Fire Danger Rating System are obtained by grouping depth, particle size, and load into a classification scheme. Data gathered from sampling fuel arrays should characterize the horizontal pattern of differing fuel types as well as the spatial occurrence of the basic fuel properties (load, size, depth) within a fuel type. Other fuel properties--heat content, mineral content, and particle density--have little variation within the fuel type and are assumed constant. Fuel moisture is time-dependent responding to diurnal changes in humidity and temperature. However, these changes are sufficiently slow so that fuel moisture can be considered constant over the duration of the fire being examined. Although moisture can be introduced as a spatial variable, it is held constant so that the response to nonmoisture fuel variability can be emphasized. It is anticipated that experienced land managers will make adjustments for moisture changes.

Two methods of fuel assessment are presented: (1) sampling a specific size area at periodic intervals along transects, and (2) if components are random, evaluating the percent cover and describing the uniform fuel properties of each component.

SLASH

The first method stated was employed in slash owing to the absence of recognizable patterns in the spatial arrangement of the fuels. Transects were obtained from a slash area composed primarily of western larch and grand fir. The area was essentially a clearcut with only a few remaining trees. Trees were cut to an 8-inch (20 cm) unmerchantable top and the entire tree except the top skidded to the landing. Nonuniformity was assessed in terms of load and depth along a 100-foot (30.5 m) transect at 2-foot (0.61 m) intervals. The fuel load was estimated by size class from the number of intercepts through a vertical sampling plane (Brown 1974). The following size classes were assessed: 1h, 10h, and 100h.[2] Pieces greater than 3 inches in diameter were measured but not considered in the model because they do not significantly contribute to fire spread.

---

[2]Fuel size classes are characterized by the time lag constant related to their ability to respond to humidity by absorbing or desorbing moisture (Fosberg 1970). The 0-1/4 inch (0-0.63 cm) size class is called 1h, 1/4-1 inch (0.64-2.54 cm) the 10h, and the 1-3 inch (2.55-7.62 cm) the 100h.

Because of the roughness of the surface of slash, it was necessary to define a depth called the bulk depth. It is an estimated mean that retains the bulk density of the inventoried fuel load and is confined to a cylinder 1 foot (0.30 m) in radius whose central axis is perpendicular to the slope at the sample point. Four estimates are made within the cylinder, each representative of 25 percent of the area (not necessarily a quadrant). Vertical gaps of more than 1 foot are subtracted before each estimate is completed. Gaps less than 1 foot are assumed to maintain vertical continuity through the potential flame height. The average of the four estimates is recorded as the estimated mean depth.

Each logged unit was measured in two stages. A grid of approximately 30 sample plots was established for each unit. In the first stage, the load for each of the four size classes was measured at each plot according to Brown (1974). In the second stage, the unit was arbitrarily divided into four sections and a sample plot was chosen at random from each section. At the first sample plot, a 100-foot (30.5 m) transect was selected at random and oriented in one of three directions: (1) 60° counterclockwise to the uphill direction, (2) uphill, and (3) 60° clockwise from the uphill direction. A random selection of the two remaining orientations was made at the second plot. The last remaining orientation was made at the third plot. Orientation on the fourth plot was chosen at random from all three directions as in the first plot. Sample planes 2 feet (0.6 m) across were oriented first along the transect line and then perpendicular to this line with the sample point as the center. The bulk depth was recorded for each sample point (fig. 2). The 10h size class load was measured at both orientations of the sample plane at one-third of the sample points which were selected at random. The range of depths and loads obtained from transects are given in figures 3 and 4.

In stage two, only the 10h intercepts were counted. Data gathered in the first stage provide the information for relating the load in the 10h class to the other two classes (1h and 100h).

The resulting 2-foot sampling interval established a minimum cell size for the hexagonal array. A smaller size would seriously degrade the accuracy of the load estimate obtained from the planar intersect technique. If larger cells are required, they can be constructed by combining cells.

Three of the four transects taken on the slash area had similar cumulative depth distributions. The remaining transect was discarded leaving a data base of 150 bulk depths and approximately 50 10h-fuel load estimates. The unit was generally described as having a light slash load. Consequently, this unit should exhibit correspondingly low rates of spread and intensities.

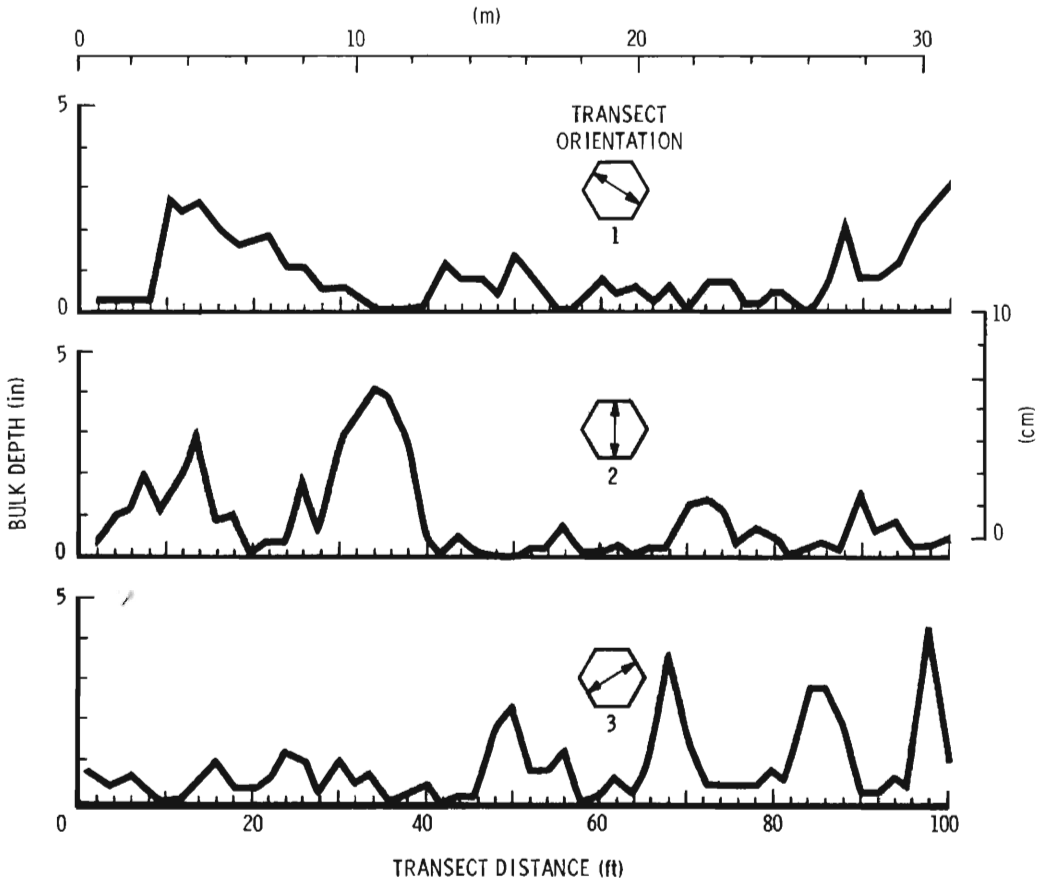

Figure 2.--A representative transect of the bulk depth evaluated every 2 feet. Three orientations are shown: (1) 60° counterclockwise to the uphill direction, (2) uphill, and (3) 60° clockwise to the uphill direction.

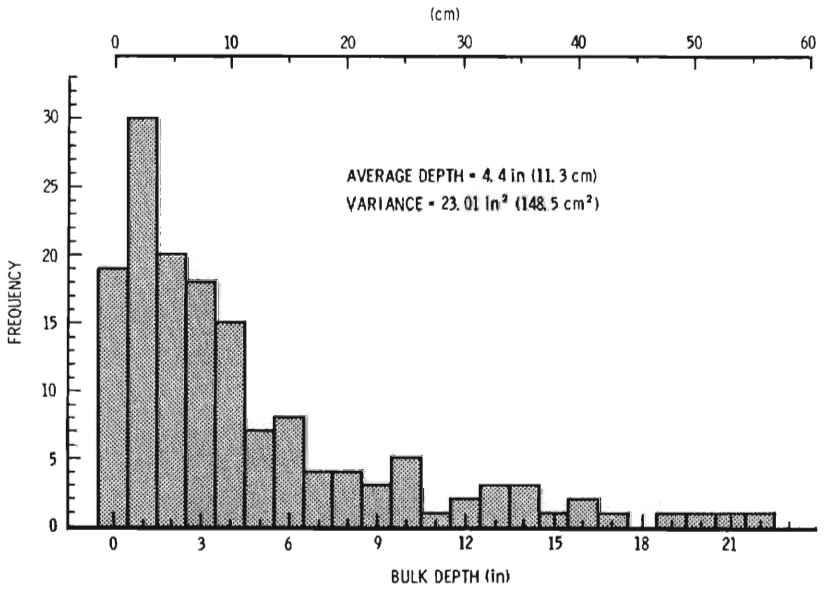

Figure 3.--Frequency distribution of the slash bulk depth. (All measurements were made at a resolution of 1 inch (2.54 cm).

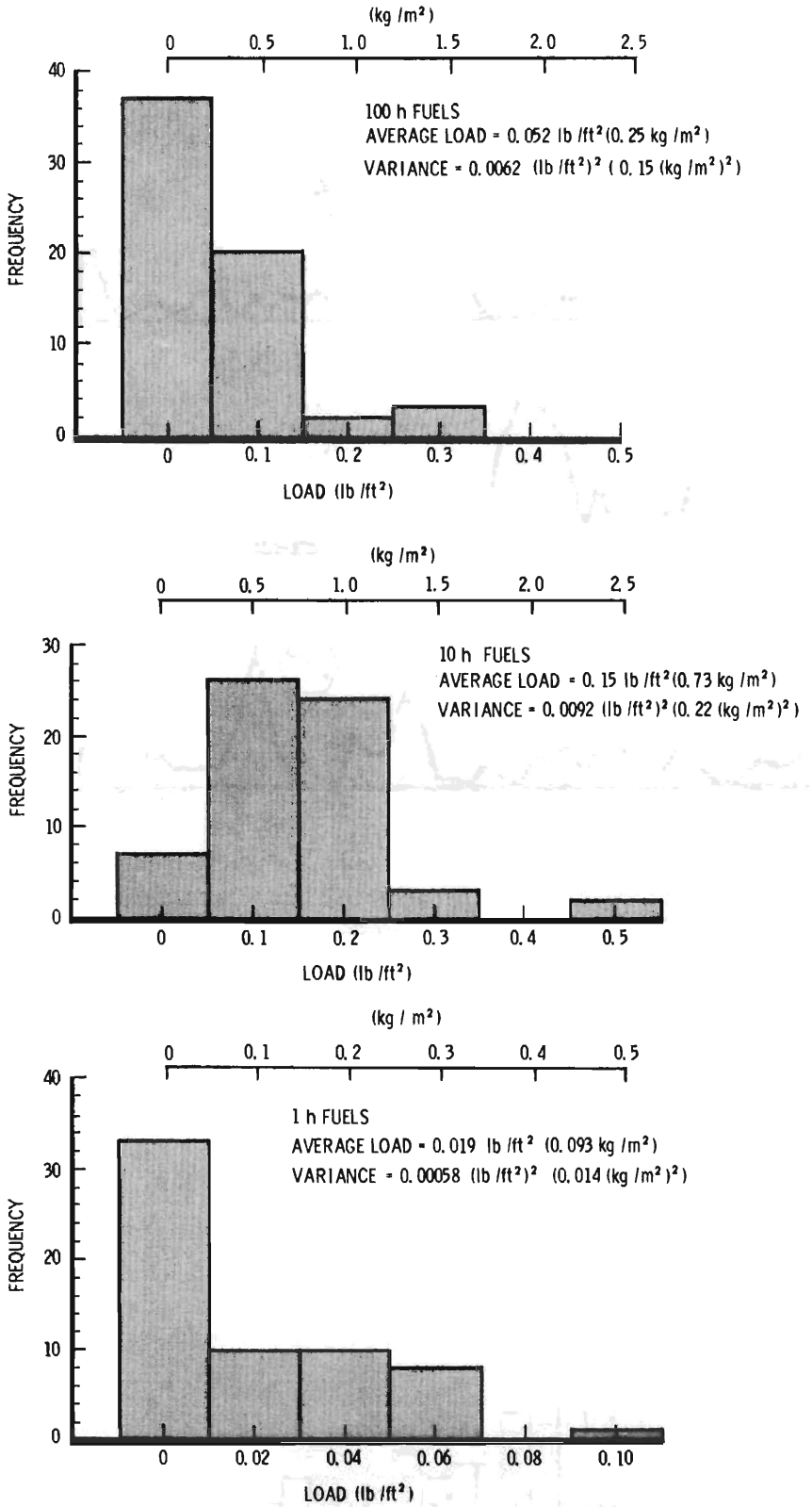

Figure 4.--Frequency distribution of the slash load. The upper distribution is for 100h fuels, the middle for 10h and the lower for 1h fuels. The implied negative load is artificial.

GRASS AND SAGEBRUSH

The second method, evaluating percent cover, was used for the mixture of grass and sagebrush because this mixture can be separated according to load breakdown by size class and depth, resulting in two components. Grass is predominantly made up of single sized particles. The bulk density, load divided by depth, varies from 0.028 to 0.085 lb/ft^3 (0.45 to 1.36 kg/m^3) with a mean of 0.05 lb/ft^3 (0.80 kg/m^3) according to data Sneeuwjagt (1974) collected from the Soil Conservation Service on Western United States grasses. A knowledge of either the load or the depth is sufficient to quantify the amount and arrangement of the grass fuel if the bulk density is known. For this example, we have considered all of the grass fuel to be dead.

Studies by Rittenhouse and Sneva (1977) and Brown (1976) allowed the evaluation of fuel loads for sagebrush according to height and largest planform diameter. The first study related the mass to the crown dimensions of the plant. The second study related the mass of single stems (including branches and foliage) to the basal diameter of the stem. But the second study (Brown 1976) went a step further to provide a breakdown of the mass by size class. Assuming that the sagebrush plant originated from a single stem. We were able to compare the two methods and obtain the load (mass per planform area) related to the crown dimensions of the plant.[3]

The following dimensions were chosen to represent sagebrush; an average height of 3 feet (91 cm) and an average diameter of 2.5 feet (76 cm). Table 1 lists the fuel parameters associated with these bulk dimensions. Fuels larger than 1/4 inch (0.64 cm) have been ignored in this analysis because they have only a minor impact on the spread rate and fireline intensity; these larger fuels are not consumed in the initial combustion process and therefore do not contribute to the spread process.

Table 1.--*Fuel parameters for grass and sagebrush*

Fuel description	Surface/volume: ft^{-1}	Surface/volume: cm^{-1}	Dry load: lb/ft^2	Dry load: kg/m^2	Moisture[1] content	Moisture of[2] extinction
Grass (fuel depth = 1.00 ft (0.30 m))						
	3000	98.4	0.0275	0.134	0.05	0.15
Sagebrush (fuel depth = 1.48 ft (0.45 m))						
Live foliage	1500	49.2	0.0538	0.263	1.00	2.00
Live 1h	677	22.2	0.0941	0.459	0.50	2.00
Dead 1h	677	22.2	0.0235	0.115	0.09	0.20

The values of fuel parameters common to all fuels discussed are:

Low heat value	8000.0 BTU/lb (18,595 kj/kg)
Particle density	32.0 lb/ft^3 (0.51 g/cm^3)
Fractional[1] mineral content	0.06
Fractional[1] effective mineral content	0.01

[1]Fraction of dryweight.

[2]A parameter involved in the computation of the moisture damping coefficient (Rothermel 1972). Higher values allow the fire to spread at higher moisture contents

[3]Data on file at the Northern Forest Fire Laboratory, Missoula, Montana.

Data collected and analyzed[3] according to Holgate (1965) shows sagebrush plants to have a random distribution. Consequently, the additional information required to fill the hexagonal fuel array is the number density of plants. The density, coupled with the average planform area, dictates the percent cover that must be achieved for a random filling of the array.

Fuel Array Generation

SLASH

Assignment of the bulk depth to each 2-foot hexagonal cell is the first step toward generating the slash fuel array. The fuel load then can be assigned to each cell through direct and indirect relationships to the depth (see appendix III).

After surrounding the area to be simulated by a boundary of depth values having the same distribution as the array but not the spatial order, the remainder of the area can be filled with depths using a linear model suggested by Mike Marsden of the Northern Forest Fire Laboratory:

$$Y = b_o + b_1X_1 + b_2X_2 + b_3X_3 + e$$

where Y is the depth being assigned to a cell and X_1, X_2, and X_3 are the depths that have been assigned to three adjacent cells and e is the error.

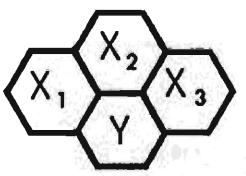

The dependent variable, Y, and independent variables, X's, change as the array is filled. A more extensive array using the same principle is shown below.

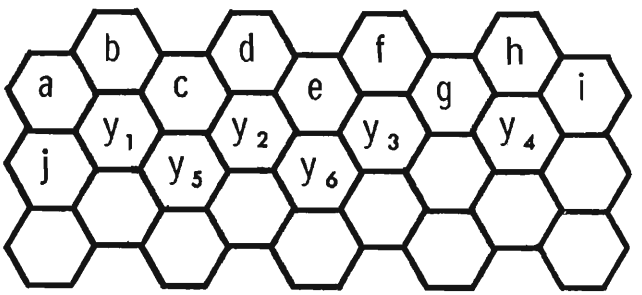

Y	:	X_1	:	X_2	:	X_3
y_1		a		b		c
y_2		c		d		e
y_3		e		f		g
y_4		g		h		i
y_5		y_1		c		y_2
y_6		y_2		e		y_3

The coefficients b_o, b_1, b_2, and b_3 are derived from the mean bulk depth and serial correlations of lags 1 and 2 of the bulk depths along linear transects through the slash array (appendix IV) and not according to the cell filling format, shown above. The following data were obtained from field transects and are used to develop the array for the slash example.

Average depth = 4.44 in (11.3 cm)

Variance = 23.01 in^2 (148.5 cm^2)

	Serial correlations	
Orientation	Lag 1	Lag 2
1	0.45	-0.044
2	0.69	--
3	0.62	+0.38

Serial correlations are simply correlations of data pairs (Snedecor and Cochran 1967) obtained from sequential transect depths of lag 1 and 2. A lag of 1 designates a correlation of adjacent depths, whereas a lag of 2 designates a correlation of data pairs obtained by skipping one depth in the transect sequence. The numerical value of the correlation is the correlation coefficient that allows the user to quantify the similarity or dissimilarity of these data pairs.

The error, e, associated with each prediction of y is obtained through random access of the cumulative distribution of the bulk depth (see appendix V). Because of the error term, generated fuel arrays are not identical. This is in agreement with the goal to produce a pattern that has the essence of the array but is not an exact reproduction. An example is wallpaper design. Your eye recognizes a pattern, but may not find exact comparison.

The average fuel parameters of the simulated fuel array are given in table 2. A comparison with figures 3 and 4 shows the tabular load and depth values to be within one standard deviation of the averages given in the figures except for 100h fuels. The foliage load is not given as a distribution. The foliage load is a fraction of the sum of the 1h, 10h, and 100h fuel loads (appendix III). The simulated serial correlations of the depth for lag 1 were 0.12, 0.31, and 0.11 for orientations 1, 2, and 3, respectively. These correlations are reduced considerably from the original correlations used to generate the fuel array. However, these correlation data showed the best comparison while maintaining an average depth comparable to the original data. Other correlations can be obtained by manipulation of the error function, but this in turn causes unacceptable changes in the average depth and its variance. The average depth of the final simulated array is 5.45 inches (13.8 cm) with a variance of 18.03 in^2 (116.3 cm^2). These data are in good agreement with the original depth data used to generate the fuel array.

Table 2.--*Average fuel parameters for slash*

Fuel description	Surface/volume: ft^{-1}	Surface/volume: cm^{-1}	Dry load: lb/ft^2	Dry load: kg/m^2	Moisture[1] content
Slash (fuel depth = 0.43 ft (0.13 m))					
Dead foliage	2000	65.6	0.118	0.576	0.05
Dead 1h	436	14.3	0.0363	0.177	0.05
Dead 10h	91	3.0	0.246	1.199	0.05
Dead 100h	29	1.0	0.190	0.926	0.05
Moisture of extinction = 0.25					

[1]Fraction of dryweight.

GRASS AND SAGEBRUSH

Generation of the grass and sagebrush fuel array is less complicated than generation of the slash fuel array because of the random distribution of the sagebrush plants within the grass matrix. The cell size of the fuel array is chosen to approximate the average diameter of the sagebrush plant, 2.5 feet (76 cm). It is necessary then only to classify the cells randomly as grass or sagebrush from a distribution that reflects the percent cover of the sagebrush within the grass matrix. A value of 30 percent was chosen as representative of the percent cover of sagebrush. Cells were assigned a fuel type of either grass or sagebrush. The fuel descriptors are given in table 1. The fuel depth listed for sagebrush is an equivalent height that when divided into the fuel load gives a bulk density equivalent to the shrub crown.

RESULTS

Predictions of the fire spread rate and intensity were obtained for slash at 0 and 2 mi/h (0 and 3.2 km/h) and for the grass-sagebrush mixture in the absence of wind. Slope was 0 for both examples and the wind was perpendicular to the initial line source. The important difference from other forms of the result is that the predictions are presented as distributions.

The rate of spread distribution was obtained from the distance traveled in a specified time along each column of cells perpendicular to the initial fire front (fig. 1). Furthermore, the characteristic distance that the fire has traveled through a cell--and thus the fraction consumed--can be calculated at a given time (appendix II). Consequently, the accuracy of the overall distance traveled is not limited to the cell size.

The predicted intensity, Byram's fireline intensity, is presented as a distribution made up of the intensities from each column of the array.

SLASH

The distributions of the rates of spread at 0 windspeed and at a 2 mi/h windspeed and 0 slope are given in figure 5. A prediction of the rate of spread assuming a uniform fuel array having the average fuel parameters of the simulated array as given in table 2 is presented also for comparison to the distribution. The average spread rate of the uniform model lies 31 percent[4] below the nonuniform model (average of the distribution) at a 0 mi/h windspeed and 21 percent below at a windspeed of 2 mi/h. The overall range for both cases lies from 65 percent below to 76 percent above the nonuniform model average.

[4]The nonuniform model average was used as the base for all percentage calculations.

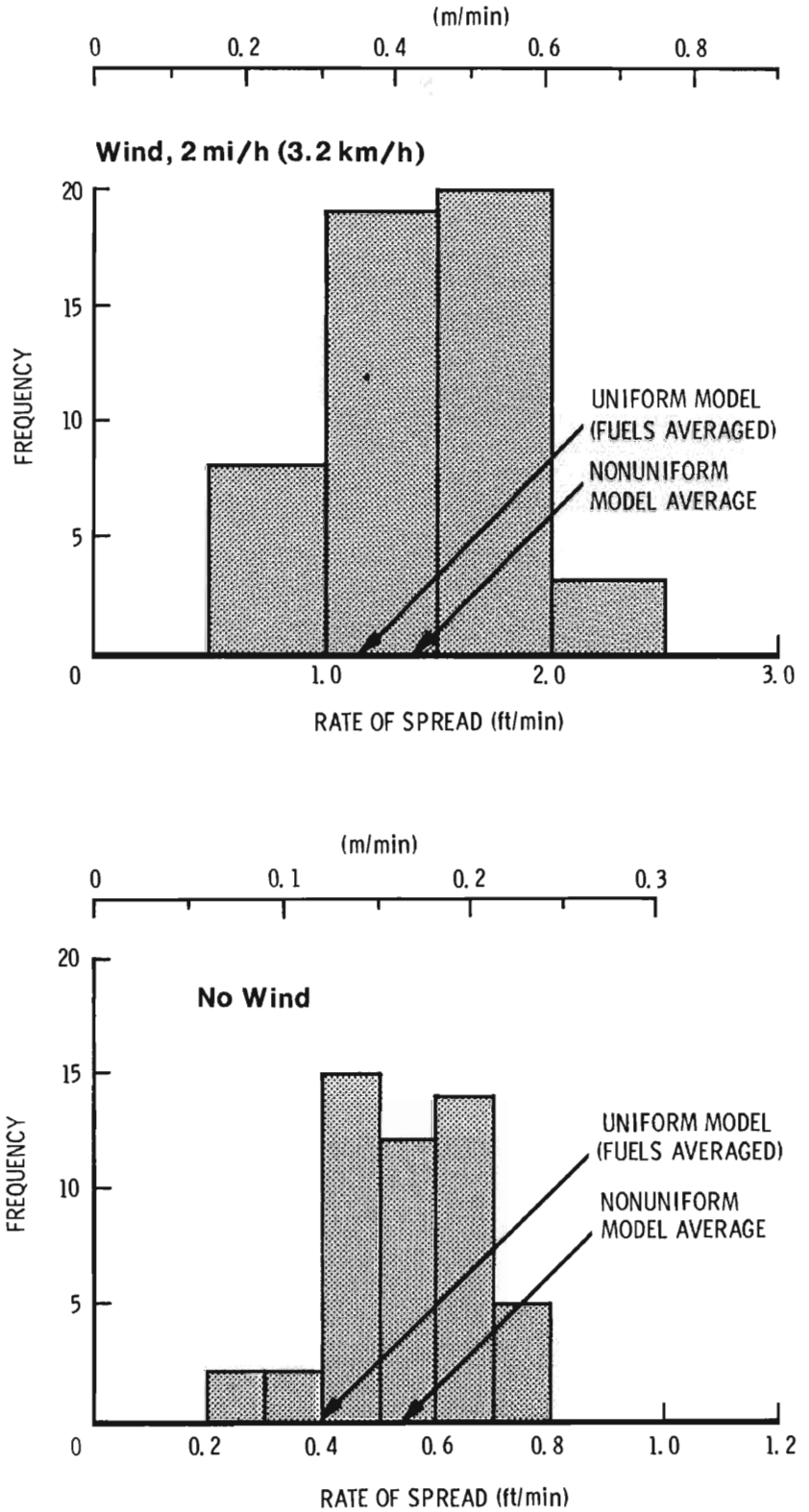

Figure 5.--Frequency distribution of the rate of spread in slash fuels at 0 windspeed and at a 2 mi/h windspeed. The average rate of spread is indicated for the uniform model (average fuel parameters from the simulated array) for comparison with the nonuniform model (average value of the distribution).

The distributions of the fireline intensities at 0 windspeed and at a 2 mi/h windspeed and 0 slope are given in figure 6. A prediction of the intensity from uniform fuel properties is again presented for comparison, similar to the presentation of the rate of spread prediction. The average intensity of the uniform model lies 43 percent above the nonuniform model at 0 mi/h windspeed and 29 percent above at 2 mi/h. Both distributions decrease monotonically with increasing intensity and are bounded on the low side by 0 intensity. The upper limit is 6 times the nonuniformity model average at 0 mi/h windspeed and 7 times that average at 2 mi/h.

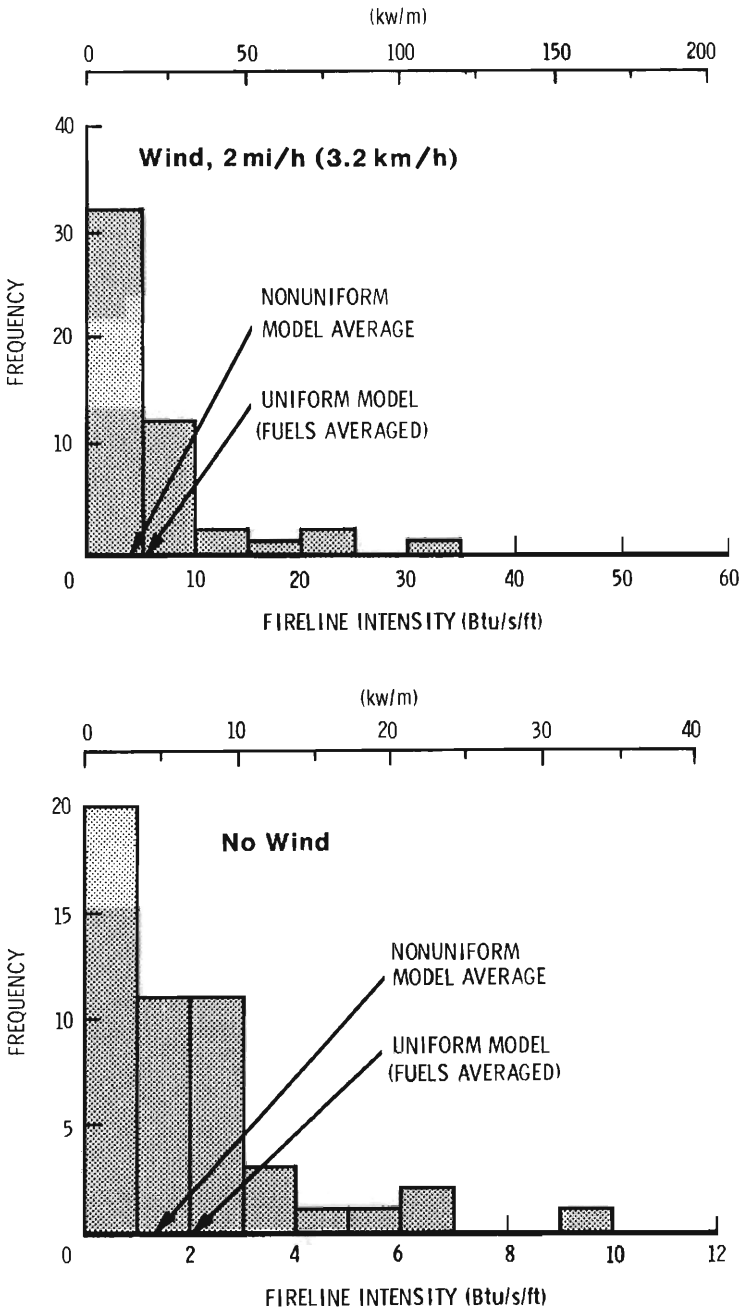

Figure 6.--Frequency distribution of fireline intensity in slash fuels (0 windspeed and 2 mi/h windspeed).

GRASS AND SAGEBRUSH

The distribution of the rate of spread in the absence of wind and slope is given in figure 7. Uniform model predictions are obtained by averaging the fuels according to the percent area covered in the fuel array. In addition to the uniform model average and the nonuniform model average, the uniform rates of spread for grass and sagebrush are given individually along with their average weighted by percent area covered. The additional predictions are possible because the fuel array is made up of two distinct components.

In addition to the uniform and nonuniform model averages as presented in figures 5 and 6, the uniform results for grass and sagebrush are indicated separately along with the average, weighted by percent area covered.

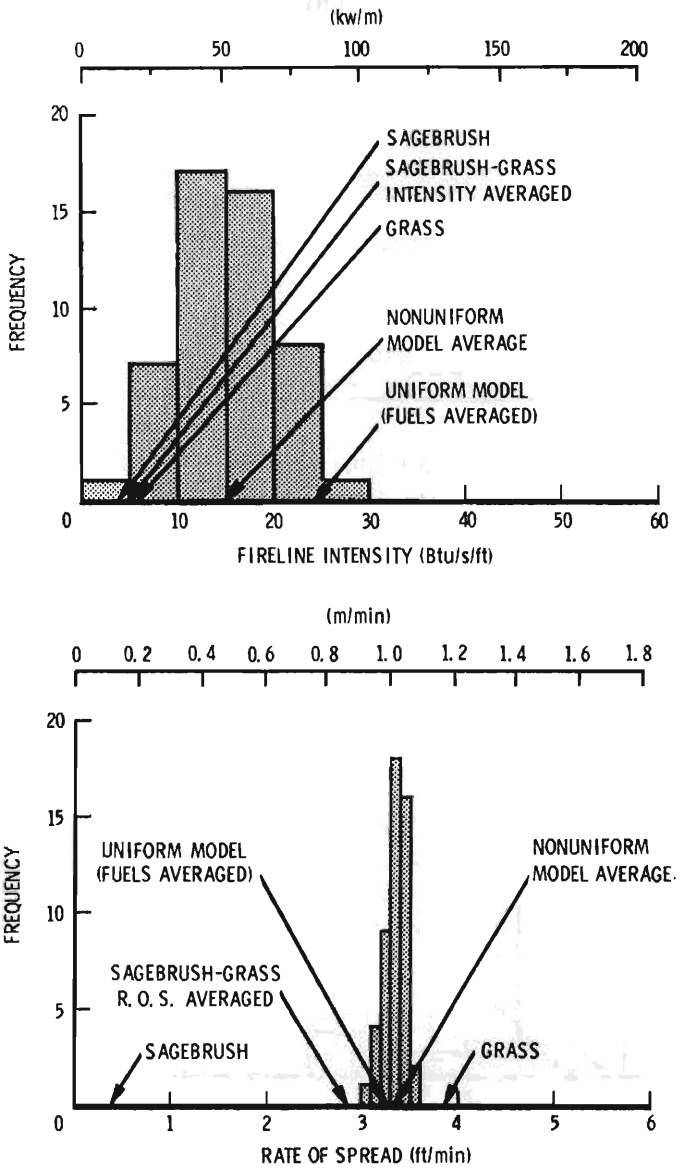

Figure 7.--Frequency distributions of rate of spread and fireline intensity in a 70 percent grass-30 percent sagebrush mixture (in absence of wind).

The rate of spread distribution lies in a narrow band near 3 ft/min. See figure 7. All values presented are less than 4 ft/min. All three averages--uniform, nonuniform, and weighted--lie within the extremes of uniform sagebrush and uniform grass.

The fireline intensity distribution extends from 0 to 30 BTU/s/ft and includes the uniform model averages. In contrast to the rate of spread, both the uniform and nonuniform model averages lie outside the extremes of uniform sagebrush and uniform grass--exceeding both values.

Fires were not simulated in the grass-sagebrush mixture at 2 mi/h windspeeds because the transition zone depth exceeded the cell size, 2.5 ft (76 cm). See appendix I. The grouping of cells into larger cells is possible but in this case the fundamental cell is the size of a sagebrush plant. Averaging such dissimilar fuel cells at this time does not serve the purpose of this paper--to illustrate the nonuniform modeling approach and the form of the result.

DISCUSSION

Fuel nonuniformities, and resulting nonuniform fire behavior, although recognized as a problem, have been ignored because of a general inability to handle nonuniformity both in its assessment and simulation and in the form of the result. Historically we have attributed a single rate of spread to a unit of land. This concept existed before the formulation of the uniform fire spread model (Rothermel 1972). The assumption of uniformity in the first attempts to describe firespread in wildland fuels was a logical first step. The assumption may have enforced our view of single valued results but is not the source of that viewpoint. The recognition of fuel nonuniformity carries with it the realization that fire exhibits nonuniform behavior. Consequently the result must be in the form of distributions, excursions about the average.

Two fuel arrays, slash and a grass-sagebrush mixture, are presented as examples for describing the nonuniform fire behavior model. Slash is a single fuel type with varying depth and load. The grass-sagebrush mixture is a mixture of fuel types. Unlike slash, most any location in the mixture has a dichotomous description as either grass or sagebrush.

All possible combinations of obtaining average fire behavior results using the uniform fire model were employed for comparison with the distributions. For slash, the average depth and fuel load were used. For the grass-sagebrush mixture, there were the additional results obtained from uniform grass, uniform sagebrush, weighted average of grass and sagebrush fuels, and the weighted average of the two results for uniform grass and uniform sagebrush.

In general, there is agreement among the averages of the uniform model (fuel parameters averaged) and the nonuniform model (distribution averaged). The trend indicates that the uniform model average is less than the nonuniform model for rate of spread but greater for fireline intensity. The higher frequency of zero fireline intensity in slash is attributed to the frequency of cells not having fuel. This is consistent with the grass-sagebrush mixture results where empty cells were not present.

The average fireline intensities of the slash are low values that suggest a minimum capability to spread fire. However, the distribution indicates that portions of the fire at a 2 mi/h windspeed would be comparable to a prescribed litter fire but would be easy to control. The last statement illustrates the importance of the distribution. Although the results are not alarming, a single average value even if correct does not indicate the upper limits of the intensity.

The upper limit on windspeed can be overcome by averaging cells into larger cells so that the influence of the fire from one cell does not extend beyond adjacent cells. This is in keeping with the relative reduction in the influence of spatial variations in fuel as the flame increases in response to wind. Future applications will likely employ general fuel models having flexibility in resolution as needs arise.[5]

The form of the result offers new ways of presenting alternatives to the land manager. With a distribution of results it is possible to ask what the probability is that a given range of rate of spread or intensity will occur. A high rate of spread or intensity although having a low probability may be intolerable. Viewing fire behavior in the form of probabilities gives a more accurate description of the probable fire behavior and a reasonable basis for management decisions.

PUBLICATIONS CITED

Albini, Frank A.
1976. Estimating wildfire behavior and effects. USDA For. Serv. Gen. Tech. Rep. INT-30. Intermt. For. and Range Exp. Stn., Ogden, Utah.

Anderson, Hal E.
1968. Fire spread and flame shape. Fire Tech. 4(1):51-58.

Anderson, Hal E.
1969. Heat transfer and fire spread. USDA For. Serv. Res. Pap. INT-69, 20 p. Intermt. For. and Range Exp. Stn., Ogden, Utah.

Brown, James K.
1966. Quantitative description of the physical properties of forest fuels. Problem Analysis Fuels Science Project 2104, NFFL, Missoula, Montana.

Brown, James K.
1974. Handbook for inventorying downed woody material. USDA For. Serv. Gen. Tech. Rep. INT-16. Intermt. For. and Range Exp. Stn., Ogden, Utah.

---

[5]Pursuing extended application of this model at this time detracts from the main purpose of explaining the model.

Brown, James K.
1976. Estimating shrub biomass from basal stem diameters. Can. J. For. Res. 6(2):153-158.
Daubenmire, R. and Jean B. Daubenmire.
1968. Forest vegetation of Eastern Washington and Northern Idaho. Washington Agric. Exp. Stn., College of Agriculture, Washington State University Tech. Bull. 60.
Davis, Kenneth P.
1959. Forest fire control and use. McGraw-Hill.
Dijkstra, E. W.
1959. A note on two problems in connexion with graphs. Numer. Math. 1:269-271.
Fons, W.
1946. Analysis of fire spread in light forest fuels. J. Agr. Res. 72(3):93-121, illus.
Fosberg, Michael.
1970. Drying rates of heartwood below fiber saturation. For. Sci. 16:57-63.
Frandsen, William H.
1971. Fire spread through porous fuels from the conservation of energy. Combus. and Flame 16:9-16, illus.
Holgate, P.
1965. Some new tests of randomness. J. of Ecol. 53:261-266.
Kendall, M. G. and A. Stuart.
1967. The advanced theory of statistics. Vol. 2, p. 334-335. Hafner.
Kourtz, Peter H. and William G. O'Regan.
1971. A model for a small forest fire--to simulate burned and burning areas for use in a detection model. For. Sci. 17:163-169.
Rittenhouse, L. R. and F. A. Sneva.
1977. A technique for estimating big sagebrush production. J. of Range Mgmt. 30(1).
Rothermel, Richard C.
1972. A mathematical model for predicting fire spread in wildland fuels. USDA For. Serv. Res. Pap. INT-115, 40 p. Intermt. For. and Range Exp. Stn., Ogden, Utah.
Rothermel, Richard C.
1974. Concepts in fire modeling. Study Guide, Advanced Fire Management Training Course, National Wildfire Coordinating Group Training Center, Marana, AZ.
Steward, F. R.
1971. A mechanistic fire spread model. Combust. Sci. and Tech. 4:177-186.
Thomas, P. H. and D. L. Simms.
1963. Report on forest research. Her Majesty's Stationery Office, London. 108 p.

NOMENCLATURE

Symbol	*Definition*	*Units*
I_R	Reaction intensity	kw/m^2
I_B	Fireline intensity	kw/m
F	Burning fraction of cell	none
D	Cell width	m
D'	Transition distance where fire is influenced by old and new cell	m
R	Rate of spread; or, Multiple correlation coefficient in statistical analysis location	m/min none
t_d	Delay time	min
τ_r	Residence time	min
σ	Surface area-to-volume ratio	cm^{-1}
$\tilde{\sigma}$	σ value within cell weighted by total exposed surface area of each particle size	cm^{-1}
d	Particle diameter	cm
t	Time	min
R_T	Rate of spread in transition distance	m/min
ε	Effective heating number	none
Q_{ig}	Volumetric heat of preignition	kj/m^3
ξ	Propagating heat flux ratio	none
ϕ_w	Wind factor	none
ϕ_s	Slope factor	none
s	Distance fire has traveled in cell	m
f(t)	Time dependent decreasing influence from old cell	none
h(t)	Time dependent increasing influence from new cell	none
θ	Time since ignition of cell	min
e	Error term	none

APPENDIX I: DELAY TIME

The delay time of a cell is the time that must elapse from the time that the cell is ignited until it is able to ignite adjacent cells. In the simulation, we are concerned with fire behavior only at the resolution of the cell size. The fire is viewed as jumping into a cell at ignition and then waiting out the delay time before jumping into unignited adjacent cells. However, to develop a method of calculating delay time, the behavior of the fire within a cell must be considered.

After cell (i+1) is ignited by cell i, the fire spreads a transition distance, D', before it reaches a quasi-steady state. During the time that it takes the fire to spread this distance, the influence of cell i is decreasing and the influence of cell (i+1) is increasing. The fire spreads the remainder of the distance through (i+1) at a rate which is calculated according to the uniform fire spread model (Rothermel 1972).

The delay time is expressed as the sum of the residence time and the time that it takes the fire to spread the remaining distance (D-D') at a uniform rate:

$$t_d = (\tau_r)_{i+1} + (D - D')/R_{i+1}$$

where

$(\tau_r)_{i+1}$ = residence of cell (i+1)

D = cell width

D' = transition distance

R_{i+1} = quasi-steady state rate of spread in cell (i+1).

The residence time, $(\tau_r)_{i+1}$, is the amount of time that fire exists at a given point as it spreads through a fuel array. Residence time is assumed to be a measure of the time that it takes a fire in cell (i+1) to achieve the quasi-steady state where it is no longer influenced by cell i and spreads at a rate dependent only on the fuel parameters of cell (i+1). Our goal in constructing the hexagonal fuel array is to choose the cell size such that the time for the fire to spread through the cell is greater than the characteristic residence time of the fuel particles in cell (i+1).

The residence time is expressed as the ratio of the combustion zone depth (approximately the horizontal region of active flaming) to the rate of spread. Anderson (1969) found the following approximation for the residence time in terms of the particle diameter d:

$$\tau_r = 3.15d$$

where τ_r is in minutes and d is in cm. The diameter, d, can be expressed in terms of the surface area-to-volume ratio:

$$d = 4/\sigma.$$

Therefore, residence time can be calculated from the characteristic surface area-to-volume ratio:

$$\tau_r = 12.6/\tilde{\sigma}$$

where $\tilde{\sigma}$ has the units of cm^{-1}.

Each hexagonal cell has a characteristic surface area-to-volume ratio obtained from the average particle diameter weighted by the total exposed surface area of each size class of fuels within the cell (Rothermel 1972). Thus, the residence time is an average property of the cell.

The values required for each cell for the delay time calculation are I_R, εQ_{ig}, ξ, ϕ_w, ϕ_s, and τ_r. These values are calculated in turn from measurable fuel properties. The reaction intensity, I_R, may be thought of as the "heat source" affecting adjacent cells. The second term, εQ_{ig}, is the product of the effective heating number, ε, and the volumetric heat of preignition, Q_{ig}. This term may be thought of as the "heat sink," the absorption of heat required for the fire to advance into the cell. The propagating flux ratio, ξ, is the heat coupling coefficient operating on the reaction intensity to obtain the propagating flux. The wind and slope factors, ϕ_w and ϕ_s, are used along with the direction of spread in relation to the directions of the wind and slope to calculate a wind-slope factor, $g(\phi_w,\phi_s)$.[6] Calculation of I_R, εQ_{ig}, ξ, ϕ_w, and ϕ_s is described in Rothermel (1972).

The rate of spread in cell (i+1) is initially influenced by the cell i. The fire is assumed to have achieved a quasi-steady state when the residence time of cell (i+1) has elapsed. To smooth the change in rate of spread within cell (i+1), a gradual change is assumed. Two possible cases must be considered: I. $(\tau_r)_i \leq (\tau_r)_{i+1}$, and II. $(\tau_r)_i > (\tau_r)_{i+1}$. For case I the influence of cell i terminates at time $(\tau_r)_i$. The influence of cell (i+1) continues increasing until time $(\tau_r)_{i+1}$ when the fire reaches its quasi-steady state. For case II the influence of cell i is terminated at time $(\tau_r)_{i+1}$ rather than $(\tau_r)_i$. At $(\tau_r)_{i+1}$ the rear of the combustion zone leaves the boundary between the cells producing a burned out area between the cells whereupon cell i is assumed to no longer influence cell (i+1). Frank Albini of the Northern Forest Fire Laboratory suggested the following mathematical model for expressing these influences.

The distance, s, that the fire has traveled in cell (i+1) by time t is:

Case I: $(\tau_r)_i \leq (\tau_r)_{i+1}$

$$s = R_T \int_0^t f_1(t)dt + R_{i+1} \int_0^t h(t)dt \qquad (2)$$

---

[6]Albini, see footnote 1.

Case II: $(\tau_r)_i > (\tau_r)_{i+1}$

$$s = R_T \int_0^t f_2(t)dt + R_{i+1} \int_0^t h(t)dt \tag{3}$$

where

$$f_1(t) = \begin{cases} 1 - t/(\tau_r)_i & \text{for } t \leq (\tau_r)_i \\ 0 & \text{for } t > (\tau_r)_i \end{cases} \tag{4}$$

$$f_2(t) = \begin{cases} 1 - t/(\tau_r)_{i+1} & \text{for } t \leq (\tau_r)_{i+1} \\ 0 & \text{for } t > (\tau_r)_{i+1} \end{cases} \tag{5}$$

$$h(t) = \begin{cases} t/(\tau_r)_{i+1} & \text{for } t \leq (\tau_r)_{i+1} \\ 1 & \text{for } t > (\tau_r)_{i+1} \end{cases} \tag{6}$$

t = time since ignition of cell (i+1)

$(\tau_r)_i$ = residence time of cell i

$(\tau_r)_{i+1}$ = residence time of cell (i+1)

R_T = rate of spread as the fire passes from cell i to cell (i+1)

R_{i+1} = quasi-steady state rate of spread in cell (i+1).

The terms $f_1(t)$ and $f_2(t)$ are time dependent decreasing influences from cell i while h(t) is a time dependent increasing influence from cell (i+1).

A graphical representation of the "influence" factors $f_1(t)$, $f_2(t)$, and h(t) are given in figure 8.

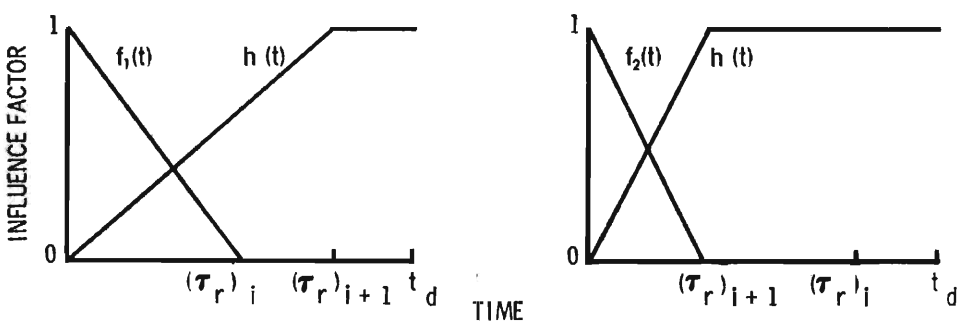

Figure 8.--Influencing factors governing fire transition from cell i to cell (i+1)

The quasi-steady rate of spread for cell (i+1) is calculated as described by Rothermel (1972):

$$R_{i+1} = (I_R)_{i+1} g_{i+1}(\phi_w, \phi_s) \xi_{i+1} / (\varepsilon Q_{ig})_{i+1}. \tag{7}$$

The transition rate of spread as the fire moves from cell i into cell (i+1) is calculated from the heat source terms of cell i and the absorption terms of cell (i+1):

$$R_T = (I_R)_i g_i(\phi_w, \phi_s) \xi_{i+1} / (\varepsilon Q_{ig})_{i+1}.$$

This can also be written as:

$$R_T = CR_{i+1} \tag{8}$$

where

$$C = (I_R)_i g_i(\phi_w, \phi_s) / (I_R)_{i+1} g_{i+1}(\phi_w, \phi_s).$$

Substituting equations (7) and (8) into equations (2) and (3) and evaluating the integrals over the intervals illustrated in figure 8, the distance that the fire spreads into a cell in a given time is as follows:

Case I: $(\tau_r)_i \leq (\tau_r)_{i+1}$

$$s = \begin{cases} CR\left(t - t^2/2(\tau_r)_i\right) + R\left(t^2/2(\tau_r)_{i+1}\right), & \text{for } 0 < t \leq (\tau_r)_i \quad (9a) \\ CR(\tau_r)_i/2 + R\left(t^2/2(\tau_r)_{i+1}\right), & \text{for } (\tau_r)_i < t \leq (\tau_r)_{i+1} \quad (9b) \\ D' + \left(t - (\tau_r)_{i+1}\right)R, & \text{for } (\tau_r)_{i+1} < t < t_d \quad (9c) \end{cases}$$

Case II: $(\tau_r)_i > (\tau_r)_{i+1}$

$$s = \begin{cases} CR\left(t - t^2/2(\tau_r)_{i+1}\right) + R\left(t^2/2(\tau_r)_{i+1}\right), & \text{for } 0 < t \leq (\tau_r)_{i+1} \quad (10a) \\ D' + \left(t - (\tau_r)_{i+1}\right)R, & \text{for } (\tau_r)_{i+1} < t \leq t_d \quad (10b) \end{cases}$$

where $R = R_{i+1}$.

The transition distance, D', can be obtained by solving equations (9b) and (10a) at $t = (\tau_r)_{i+1}$.

Case I: $(\tau_r)_i \leq (\tau_r)_{i+1}$

$$D' = R\left(C(\tau_r)_i + (\tau_r)_{i+1}\right)/2 \tag{11}$$

Case II: $(\tau_r)_i > (\tau_r)_{i+1}$

$$D' = R(\tau_r)_{i+1}(C + 1)/2. \tag{12}$$

Equations (9) and (10) can be solved for t to obtain the time that it takes the fire to spread a distance, s, in the cell.

Case I: $(\tau_r)_i \leq (\tau_r)_{i+1}$

$$t = \begin{cases} \left[-C + \sqrt{C^2 + 2B\left(1 - C(\tau_r)_{i+1}/(\tau_r)_i\right)}\right] \Big/ \left[1/(\tau_r)_{i+1} - C/(\tau_r)_i\right], & \text{(13a)} \\ \quad \text{for } (\tau_r)_i < (\tau_r)_{i+1} \text{ or } C \neq 1 \\ \quad \text{and } 0 < s \leq R(\tau_r)_i\left[C + (\tau_r)_i/(\tau_r)_{i+1}\right]/2 \\ s/R, \quad \text{for } (\tau_r)_i = (\tau_r)_{i+1},\ C = 1 & \text{(13b)} \\ \quad \text{and } 0 < s \leq R(\tau_r)_i \\ \sqrt{2s(\tau_r)_{i+1}/R - C(\tau_r)_i(\tau_r)_{i+1}}, & \text{(13c)} \\ \quad \text{for } R(\tau_r)_i\left[C + (\tau_r)_i/(\tau_r)_{i+1}\right]/2 < s \leq D' \\ (s - D')/R + (\tau_r)_{i+1}, & \text{(13d)} \\ \quad \text{for } D' < s \leq D \end{cases}$$

Case II: $(\tau_r)_i > (\tau_r)_{i+1}$

$$t = \begin{cases} \left[-C + \sqrt{C^2 + 2B(1 - C)}\right] \Big/ \left[(1 - C)(\tau_r)_{i+1}\right], & \text{for } 0 < s \leq D' \quad \text{(14a)} \\ (s - D')/R + (\tau_r)_{i+1}, & \text{for } D' < s \leq D \quad \text{(14b)} \end{cases}$$

where

$$R = R_{i+1}$$

$$B = s/R(\tau_r)_{i+1}.$$

If the fire reaches its quasi-steady state in a cell, equation (13c) or (14b) for s = D is equivalent to finding the delay time as described in equation (1).

As stated earlier, the cell size should be large enough for the fire to achieve a quasi-steady state in every cell. Otherwise, the influence of cell i would extend beyond cell (i+1). At present the algorithm does not handle this situation. Increasing the cell size excessively may result in averaging out the nonuniformities we originally intended to examine. It is essential to design the array so that a high percentage of the hexagonal cells achieve a quasi-steady state rate of spread and accept the small error resulting from the few exceptions. If the calculated transition distance is larger than the cell size (D' > D), the delay time is calculated as the time that it takes the fire to travel the distance D.

The following is a general procedure for obtaining the delay time. If $(\tau_r)_i \leq (\tau_r)_{i+1}$, substitute D for s, select the equation having the correct limits from equations 13a, b, or c, and solve for t. If $(\tau_r)_i > (\tau_r)_{i+1}$, proceed in the same manner using equation 14a or b.

APPENDIX II: CELL BURNING FRACTION

The fraction of a cell that is burning at time θ since its ignition is evaluated from the distance equations for s in appendix I. Initially the front of the burning zone spreads into the cell as described by s with $t = \theta$. The rear of the burning zone follows in the same manner but with $t = \theta - \tau_r$, where τ_r is the residence time in the cell. During passage of the fire, the front and the rear of the burning zone may exist in the cell together, separately, or be absent. The following equations account for all cases:

$F = 0$	for $\theta \leq 0$	The cell has not been ignited.
$F = s(\theta)/D$	for $D' \leq D$ and $0 < \theta \leq \tau_r$	The fire front is in the cell. There is no burned out area.
	or for $D' > D$ and $0 < \theta \leq t_d$	
$F = (s(\theta) - s(\theta - \tau_r))/D$	for $D' \leq D$ and $\tau_r < \theta \leq t_d$	Both the fire front and rear are in the cell.
$F = 1$	for $D' > D$ and $t_d < \theta \leq \tau_r$	The entire cell is burning.
$F = 1 - s(\theta - \tau_r)/D$	for $D' \leq D$ and $t_d < \theta \leq t_d + \tau_r$	The fire front has passed the cell.
	or for $D' > D$ and $\tau_r < \theta \leq t_d + \tau_r$	There is a burned out area.
$F = 0$	for $\theta > t_d + \tau_r$	The cell is burned out.

where

F = fraction of the cell that is burning at time θ

D = cell size

D' = transition distance

t_d = delay time

τ_r = cell residence time

$s(\theta)$ = distance the front of the burning zone has spread at time $t = \theta$ according to equation 9 or 10

$s(\theta - \tau_r)$ = distance the rear of the burning zone has spread at time $t = \theta - \tau_r$ according to equation 9 or 10.

APPENDIX III: CELL LOAD EVALUATION

The 10h load is assigned through a relationship between the load and depth. The 1h and 100h are then assigned through two separate relationships of each of these loads to the 10h load derived from the first stage inventory. The necessary relationships are expressed in figure 9 as cumulative distributions of the following ratios: (upper) 10h load to bulk depth, (middle) 1h load to 10h, and (lower) 100h load to 10h load. For each cell in the depth array, the 10h load can be obtained by random access of the upper distribution in figure 9. The other two loads are determined in the same manner using the 10h load as a base and accessing the middle and lower distributions.

An estimate of the foliage load was made based on the dominant species composition of slash, foliage retention by these species, and a knowledge of the foliage load relative to the sum of the 1h, 10h, and 100h slash load.

Dominant species composition of the slash was western larch and grand fir. Because larch loses its needles quickly compared to grand fir and the slash had gone through one winter, it is reasonable to assume that western larch had lost all of its foliage while grand fir retained its foliage. Brown (1978) found that the grand fir foliage load was approximately 50 percent of the sum of the 1h, 10h, and 100h loads. Depending upon the relative amounts of western larch and grand fir, the foliage load could vary from zero to 50 percent of the overall sum of the 1h, 10h, and 100h slash load. An average of 25 percent was chosen. After 1h, 10h, and 100h loads are determined for each cell, 25 percent of the sum is used to represent the foliage load.

APPENDIX IV: EVALUATING b_0, b_1, b_2 AND b_3

Evaluation of the coefficients b_o, b_1, b_2, and b_3 of the multiple linear regression equation:

$$Y = b_o + b_1X_1 + b_2X_2 + b_3X_3 + e$$

is obtained by using serial correlation data and the mean and variance of the bulk depth distribution obtained from linear fuel array transects. The location of cell Y relative to cells X_1, X_2, and X_3 in the cell filling model is:

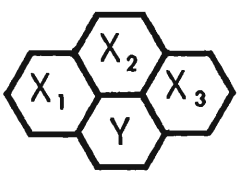

where the dependent variable, Y, is the cell being filled, and the independent variables, X_1, X_2, and X_3 are the cells already filled. It is important to distinguish between the data collected from the linear transects and the requirements of the cell filling algorithm.

Constants are added to the denominator of each ratio to avoid dividing by zero. Appropriate corrections are later made upon assignment to the cell. Metric conversion of these histograms is not given because the histograms are working tools and do not lend themselves to easy conversion.

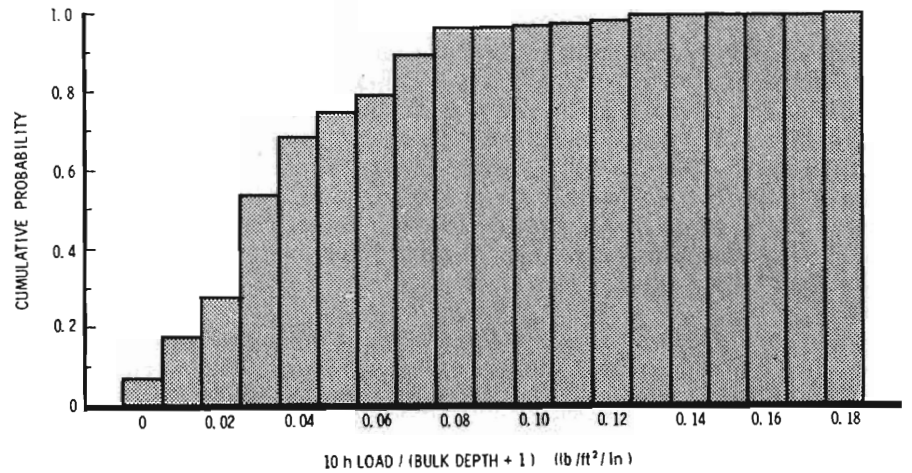

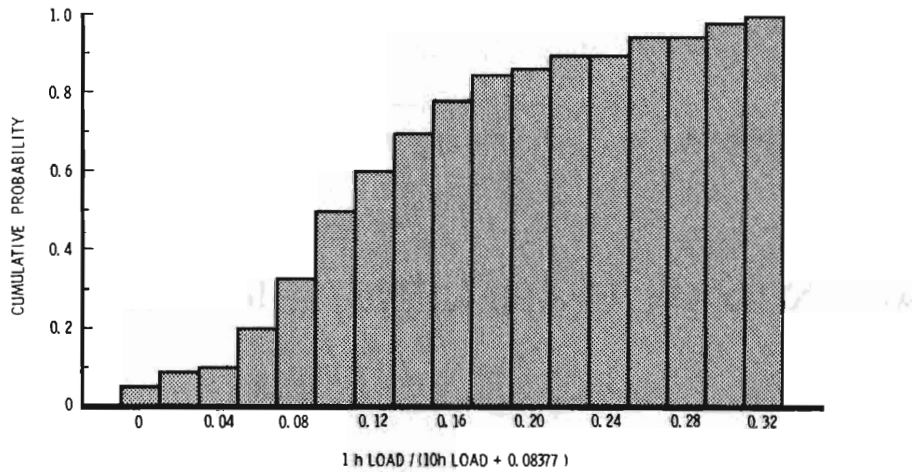

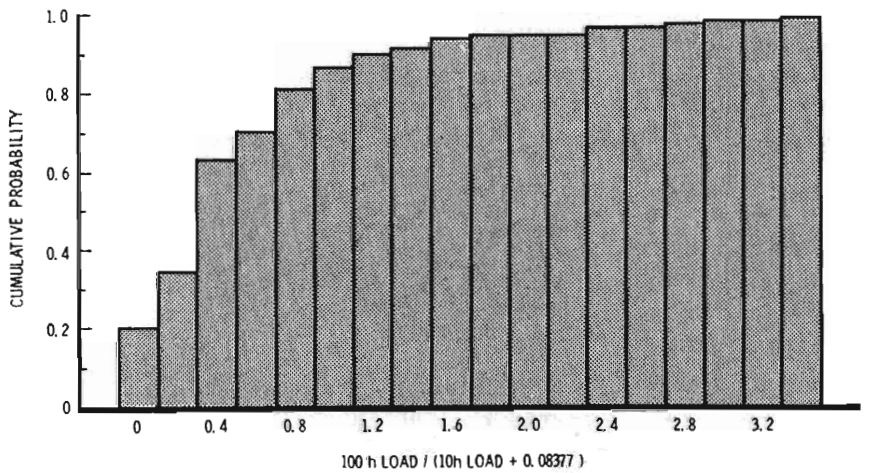

Figure 9.--Cumulative probability distributions for assigning 1h, 10h, and 100h fuel loads to each cell given the bulk depth.

The principles of multiple regression analysis are used to estimate Y from X_1, X_2, and X_3.

The following analysis is simplified by transforming X's and Y's to deviations from the mean:

$$x = X - \overline{X}$$

and

$$y = Y - \overline{Y}.$$

Normal set of equations for $Y = f(X_1, X_2, X_3) + e$ is

$$\sum x^2_{1i} b_1 + \sum x_{1i} x_{2i} b_2 + \sum x_{1i} x_{3i} b_3 = \sum x_{1i} y_i$$

$$\sum x_{2i} x_{1i} b_1 + \sum x^2_{2i} b_2 + \sum x_{2i} x_{3i} b_3 = \sum x_{2i} y_i$$

$$\sum x_{3i} x_{1i} b_1 + \sum x_{3i} x_{2i} b_2 + \sum x^2_{3i} b_3 = \sum x_{3i} y_i$$

and

$$\sum Y_i - \sum (X_{1i} b_1 + X_{2i} b_2 + X_{3i} b_3) = n b_o.$$

Note that the variables in the fourth equation are uncorrected for deviations from the mean.

The serial correlation coefficient obtained from the bulk depth transect is related to the product mean and has this relation:

$$r_{ab} = \text{cor}(x_j, x_{j+a})_b = \left[\frac{\text{cov}(x_j, x_{j+a})}{\sqrt{\text{var}(x_j)\,\text{var}(x_{j+a})}} \right]_b$$

where a is the lag and b is the orientation and have values a = 1, 2; b = 1, 2, 3. The above expression can be written:

$$r_{ab} = \left[\frac{\overline{x_j x_{j+a}}}{\sqrt{\overline{x_j^2}\ \overline{x_{j+a}^2}}} \right]_b$$

Thus

$$\left[\overline{x_j x_{j+a}} \right]_b = r_{ab} \left[\sqrt{\overline{x_j^2}\ \overline{x_{j+a}^2}} \right]_b.$$

x's and y's are interchangeable (see p. 13) as we move through array filling cells. Thus

$$\overline{x_j^2} \simeq \overline{x_{j+a}^2} \simeq \overline{x^2}$$

and

$$\left[\overline{x_j x_{j+a}}\right]_b \simeq r_{ab}\overline{x^2}.$$

The following diagram is used to determine orientation and lag of the correlation.

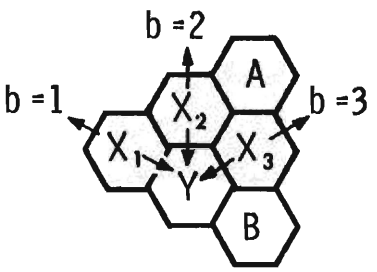

As examples, it can be seen that the correlation of cells x_2 and x_3 have orientation 1 and lag 1. The correlation of cells x_1 and A have orientation 3 and lag 2. Cells A and B are included to help in evaluating $\overline{x_{1i}x_{3i}}$. The correlation, $\overline{x_{1i}x_{3i}}$, is estimated by averaging the correlations of lag 2 illustrated by cells A and B in relation to cell X_1, because a direct estimate from the linear transect does not exist.

Since cells A and B are adjacent and directly above and below X_3, we define $\overline{x_{1i}x_{3i}}$ as:

$$\overline{x_{1i}x_{3i}} = (r_{21} + r_{23})/2.$$

Also, we can make the following observation:

$$\overline{Y}_i \simeq \overline{X}_{1i} \simeq \overline{X}_{2i} \simeq \overline{X}_{3i} \simeq \overline{X}$$

and

$$\overline{x_{1i}^2} \simeq \overline{x_{2i}^2} \simeq \overline{x_{3i}^2} \simeq \overline{x^2}.$$

We can now transform the coefficients of the b's of the normal set of equations with information gained from serial correlations along the three principle axes.

The transformed normal set of equations are below:

$$\overline{x^2}b_1 + r_{13}\overline{x^2}b_2 + \left(\frac{r_{21} + r_{23}}{2}\right)\overline{x^2}b_3 = r_{11}\overline{x^2}$$

$$r_{13}\overline{x^2}b_1 + \overline{x^2}b_2 + r_{11}\overline{x^2}b_3 = r_{12}\overline{x^2}$$

$$\left(\frac{r_{21} + r_{23}}{2}\right)\overline{x^2}b_1 + r_{11}\overline{x^2}b_2 \quad \overline{x^2}b_3 = r_{13}\overline{x^2}$$

and

$$b_o = \overline{X}(1 - b_1 - b_2 - b_3)$$

where

$\overline{x}$ = estimate of the mean bulk depth

$\overline{x^2}$ = estimate of the variance of the bulk depth.

Note that although $\overline{x^2}$ cancels in the above equations, it is retained for clarity.

Transects oriented in directions 1 and 3 should have equivalent parameters because of their symmetry about the uphill orientation (orientation 2). The following changes have been made to insure this symmetry:

$$r'_{11} = r'_{13} = (r_{11} + r_{13})/2.$$

Primes pertain to transformed new values. Theoretically, the serial correlation of lag 2 should be the square of lag 1. To insure that the two matrix elements (1,3) and (3,1) that have correlation of lag 2, $(R_{21} + R_{23})/2$, are influenced by this relation, the following change has been made:

$$(r_{21} + r_{23})/2 + \left[(r'^2_{11} + r^2_{12} + r'^2_{13})/3\right]/2 = \left[(r_{21} + r_{23})/2\right]'$$

where the second term is the mean of the squares of the three correlations of lag 1. Note that r'_{11} and r'_{13} are the new values as expressed above.

Solving the three simultaneous equations gives:

$$b_1 = b_3 = R_1(1 - r_{12})/(R_2 - 2R_1^2 + 1)$$

$$b_2 = r_{12} - 2R_1b_1$$

where

$$R_1 = (r_{11} + r_{13})/2$$

$$R_2 = (r_{21} + r_{23})/2 + (2R_1^2 + r_{12}^2)/6.$$

Rewriting for completeness

$$b_o = \overline{X}(1 - b_1 - b_2 - b_3)$$

where $\overline{X}$ is the mean bulk depth.

The coefficients of the regression equation, b_1, b_2, and b_3, depend only on the serial correlation coefficients of the slash transects (all three orientations at lag 1 and orientations 1 and 3 at lag 2). The coefficient b_o has an additional dependency on $\bar{X}$, the mean bulk depth.

APPENDIX V: ERROR TERM

The error term is derived by random access of the cumulative distribution of the bulk depth (fig. 10). Random access is achieved by entering on the y-axis of the distribution with a random number from 0 to 1. The mean bulk depth is then subtracted from the accessed bulk depth to obtain the first estimate of the error, e'. The error is further modified by taking into consideration the relation of the variance of the estimate of y, $\hat{y}$, given x, to the variance of y (Kendall and Stuart 1967):

$$s^2_{\hat{y}|x} = (1 - R^2)s^2_y$$

where R = multiple correlation coefficient.

We can write the following expression for the error by recognizing the similarity of the variance to the square of the error:

$$e = \sqrt{1 - R^2}\, e'.$$

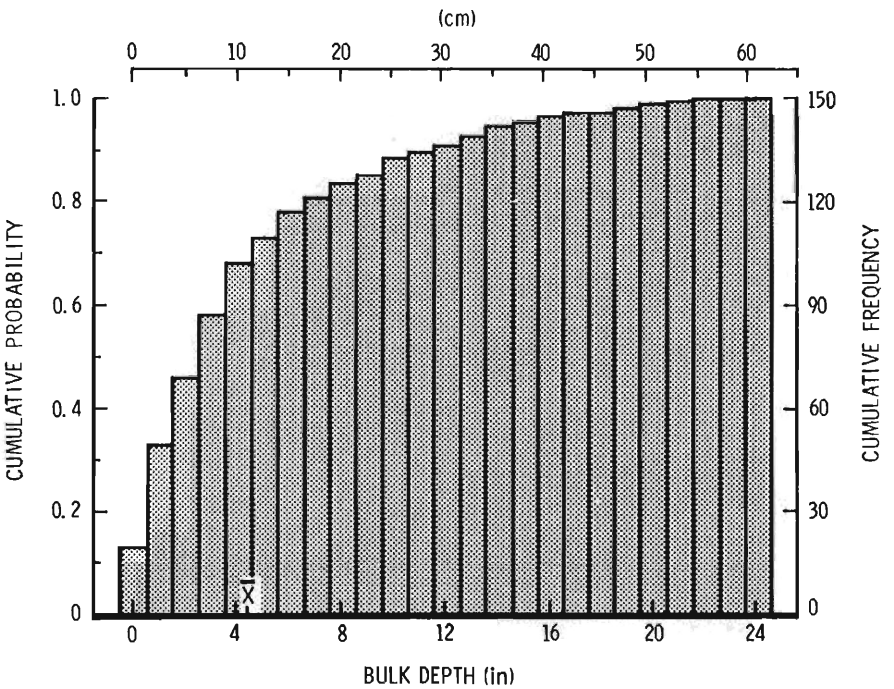

Figure 10.--Cumulative probability distribution of the bulk depth.

☆U.S. GOVERNMENT PRINTING OFFICE: 1979-0-677-019/37

Frandsen, William H., and Patricia L. Andrews.
1979. Fire behavior in nonuniform fuels. USDA For. Serv. Res. Pap. INT-232, 34 p. Intermt. For. and Range Exp. Stn., Ogden, Utah 84401.

Predicting fire behavior in nonuniform fuel arrays is a problem requiring: (1) a method of assessing fuel nonuniformity, (2) a method of simulating fuel nonuniformity, and (3) an algorithm governing fire spread through a simulated array. The bulk fuel properties (load, depth, average particle size, etc.) are partitioned into a honeycomb array. An algorithm simulates fire spread through the array by coupling predictions of heat flowing from a burning cell to predictions of the heat required for ignition of its adjacent cells. Multiple results of fire behavior are displayed as distributions in contrast to previously generated singular values. Methodology is emphasized.

KEY WORDS: fire behavior, nonuniform fuel, nonuniform fire, fire spread, fire intensity.

Frandsen, William H., and Patricia L. Andrews.
1979. Fire behavior in nonuniform fuels. USDA For. Serv. Res. Pap. INT-232, 34 p. Intermt. For. and Range Exp. Stn., Ogden, Utah 84401.

Predicting fire behavior in nonuniform fuel arrays is a problem requiring: (1) a method of assessing fuel nonuniformity, (2) a method of simulating fuel nonuniformity, and (3) an algorithm governing fire spread through a simulated array. The bulk fuel properties (load, depth, average particle size, etc.) are partitioned into a honeycomb array. An algorithm simulates fire spread through the array by coupling predictions of heat flowing from a burning cell to predictions of the heat required for ignition of its adjacent cells. Multiple results of fire behavior are displayed as distributions in contrast to previously generated singular values. Methodology is emphasized.

KEY WORDS: fire behavior, nonuniform fuel, nonuniform fire, fire spread, fire intensity.

Headquarters for the Intermountain Forest and Range Experiment Station are in Ogden, Utah. Field programs and research work units are maintained in:

Billings, Montana
Boise, Idaho
Bozeman, Montana (in cooperation with Montana State University)
Logan, Utah (in cooperation with Utah State University)
Missoula, Montana (in cooperation with University of Montana)
Moscow, Idaho (in cooperation with the University of Idaho)
Provo, Utah (in cooperation with Brigham Young University)
Reno, Nevada (in cooperation with the University of Nevada)